

Refiner: Data Refining against Gradient Leakage Attacks in Federated Learning

Mingyuan Fan¹, Cen Chen², Chengyu Wang³, Wenmeng Zhou³, Jun Huang³, Ximeng Liu¹, Wenzhong Guo¹

¹ College of Computer and Data Science, Fuzhou University, Fuzhou, China;

² School of Data Science and Engineering, East China Normal University, Shanghai, China

³ Alibaba Group, Hangzhou, China

Email: fmy2660966@gmail.com, cenchen@dase.ecnu.edu.cn, chengyu.wcy@alibaba-inc.com, wenmeng.zwm@alibaba-inc.com, huangjun.hj@alibaba-inc.com snbnix@gmail.com, guowenzhong@fzu.edu.cn

Abstract—Federated Learning (FL) is pervasive in privacy-focused IoT environments since it enables avoiding privacy leakage by training models with gradients instead of data. Recent works show the uploaded gradients can be employed to reconstruct data, i.e., gradient leakage attacks, and several defenses are designed to alleviate the risk by tweaking the gradients. However, these defenses exhibit weak resilience against threatening attacks, as the effectiveness builds upon the unrealistic assumptions that deep neural networks are simplified as linear models. In this paper, without such unrealistic assumptions, we present a novel defense, called *Refiner*, instead of perturbing gradients, which refines ground-truth data to craft robust data that yields sufficient utility but with the least amount of privacy information, and then the gradients of robust data are uploaded. To craft robust data, *Refiner* promotes the gradients of critical parameters associated with robust data to close ground-truth ones while leaving the gradients of trivial parameters to safeguard privacy. Moreover, to exploit the gradients of trivial parameters, *Refiner* utilizes a well-designed evaluation network to steer robust data far away from ground-truth data, thereby alleviating privacy leakage risk. Extensive experiments across multiple benchmark datasets demonstrate the superior defense effectiveness of *Refiner* at defending against state-of-the-art threats.

Index Terms—Federated Learning, Data Privacy, Gradient Leakage, Data Refining, Internet of Things.

I. INTRODUCTION

The Internet of Things (IoT) devices have been employed in many privacy-sensitive scenarios [1], [2] such as smart medical care [3], and collect a vast amount of data that has yet to be explored. Although deep neural networks (DNNs) emerge as a promising candidate to unleash the potential of collected data [4], [5], ever-increasing concerns for data privacy render DNNs unavailable, since collected data have to be centralized into a single data center for training DNNs [6], [7]. To avoid the requirement of transferring data outside of local devices, federated learning (FL) [8], [9] harnesses a gradient exchange mechanism to train DNNs. Specifically, as shown in Figure 1, FL alternatively executes two steps until the convergence of the shared global model [10]: 1) the central server distributes the global model to IoT devices, and 2) IoT devices upload gradients locally computed with private data (ground-truth gradients) to update the global model. However, this seemingly-reliable gradient exchange mechanism is arguably challenged by recent works [11]–[13], in which the uploaded gradients

are maliciously employed to launch gradient leakage attacks (GLA). GLA can reconstruct high-fidelity data by minimizing the distance between uploaded gradients and gradients of reconstructed data, i.e., gradient matching problems.

Over past years, several defenses [11], [14]–[16] are developed to lessen the dangers of privacy leakage raised by GLA. The core idea behind these defenses is that the high-fidelity data reconstruction power of GLA stems from the accurate gradient-to-data mapping relationship [15]. Accordingly, a natural and sensible idea is to impose subtle perturbations into ground-truth gradients so that the adversary (the server) may be obfuscated by perturbed gradients to recover false data. Crafting proper perturbations, however, is quite delicate work [15], because tiny perturbations are unable to mislead the adversary while excessive perturbations often make resultant perturbed gradients useless to the global model. Therefore, the core topic in this area is creating a better way of perturbing ground-truth gradients, i.e., crafting perturbed gradients that can sufficiently obfuscate the adversary while remaining informative as possible.

The seminal work, differential privacy [14], equally and independently perturbs each gradient element but only show negligible defense effectiveness against GLA, since both utility and privacy info included in gradient elements are not taken into account. Furthermore, pruning [11] attempts to discard the trivial gradient elements but still produces unsatisfactory defense performance, as these trivial gradients rarely involve important semantic information of original data. The state-of-the-art defense in this area is Soteria [15], which first estimates the utility and privacy info contained in each gradient element and then prunes the most cost-effective gradient elements, achieving inspiring defense performance. However, although Soteria looks impeccable, it still is broken in the latest empirical examinations [17], [18] where the adversary introduces adequate prior knowledge into the reconstruction process to compensate for the missing details, which considerably weakens the effectiveness of defenses. The major reason for Soteria being broken probably is that, the estimation method of Soteria builds upon the impractical premise [15] that DNNs can be precisely approximated by their first-order Taylor (linear) expansion. However, on the one hand, first-

order Taylor expansion only works well within a very small neighborhood surrounding original variables, and the pruning magnitude is probably to be outside the viable neighborhood [19], especially for bigger pruning ratios. On the other hand, linear expansion assumes all variables are independent of each other which is at odds with the highly non-linear and non-convex features of modern DNNs [20].

This Work. In this paper, we aim at simultaneously injecting privacy and utility info of gradients into the perturbation process, but the main difference compared with Soteria is no premise established here, which, in turn, enables us to greatly overcome the deficit of Soteria and thereby largely strengthens the defense effectiveness. Unarguably, this task is by nature highly challenging, since, without simplifying DNNs, directly deriving the analytic mapping relationship from perturbed gradients to corresponding reconstructed data is intractable, owing to the intrinsically highly non-linear and non-convex nature of DNNs [20]. Furthermore, without the explicit gradient-to-data mapping relationship, it is unclear that produced perturbations can reap how much privacy protection, i.e., the optimal perturbation direction is unknown.

To address this problem, we propose a novel approach termed as *Refiner* and the intuition behind *Refiner* stems from the fact that gradients are generated by data [7]. Inspired by the fact, instead of directly working on ground-truth gradients to craft perturbed gradients, *Refiner* refines ground-truth data to craft robust data shown in Figure 1, that contain the least privacy info yet can yield the closest utility to original ones. After getting robust data, the gradients of robust data can be served as perturbed gradients to upload. As opposed to directly explicitly optimizing gradients, *Refiner* implicitly crafts perturbed gradients with the aid of robust data. The implicit perturbation way enables us to accurately estimate the privacy info contained in perturbed gradients by plainly observing the difference between ground-truth and robust data, so as to circumvent the requirement to derive the gradient-to-data mapping relationship.

Specifically, *Refiner* crafts such robust data by jointly optimizing two metrics associated with robust data for performance maintenance and privacy protection, demonstrated in Figure 1. However, the concrete form of privacy metric is difficult to determine, due to the huge divergence between existing difference metrics [21], e.g., norm-based distances, and human-vision-system difference metrics. Particularly, Figure 2 shows that, shifting an image towards a certain direction by a unit is likely to result in non-trivial norm-based distances, but humans still perceive two images equally. To solve the problem, *Refiner* trains an evaluation network that can accurately estimate the human perception distance from robust data to the original one. The perception distance is harnessed as the privacy metric, reflecting the overall amount of disclosed privacy information regarding ground-truth data. Moreover, the performance maintenance metric is defined as the weighted distance of gradients between ground-truth and robust data. Our contributions are summarized as follows:

- We propose a novel gradient perturbation approach

named *Refiner*, where robust data is elicited to implicitly craft perturbed gradients, thereby vastly facilitating the injection of two kinds of information into perturbed gradients, compared with existing methods that directly work on gradient-truth gradients.

- We design an effective utility metric that reckons the gradient distance in a weighted fashion and the weights are determined by element-wise weight and layer-wise weight of parameters (seen in III).
- We identify the flaw of common metrics in quantifying the dissimilarity between two images, and, as a response, we suggest an evaluation network as privacy metric, which learn how to assess the dissimilarity in a manner consistent with human cognition.
- We conduct extensive experiments in multiple benchmark datasets and results against a variety of state-of-the-art attacks demonstrate that *Refiner* yields truly encouraging and promising defense effectiveness superior to existing defenses.

The remainder of this paper is organized as follows. Section II gives necessary background about the area and briefly introduces related work. Section III elaborates the proposed method *Refiner* and two metrics. Section IV conducts extensive experiments to examine the performance of *Refiner* compared with state-of-the-art defenses against various attacks. Section V concludes this paper.

II. PRELIMINARY AND RELATED WORK

In this section, we briefly introduce some necessary background and review classical works.

A. Deep Neural Network

A deep neural network generally is stacked by a series of layers, one of each is a composition of a linear function and a simple non-linear activation function [20]. Denote a deep neural network to be $F(x, \theta)$ where x and θ are input and learnable parameters of the network, respectively. To make the neural network generalize well, a common practice [20] is training the network over a dataset D , consisting of pairs of data x and corresponding label y , with a certain loss function $\mathcal{L}(\cdot, \cdot)$ and the gradient descent optimization method, known as the back propagation algorithm. The optimization detail in t -th iteration can be succinctly expressed as follow:

$$\theta_t = \theta_{t-1} - \eta \nabla_{\theta} \mathcal{L}(F(x, \theta_{t-1}), y), \quad t = 1, 2, \dots, \quad (1)$$

where the subscript of θ is used to denote timestamp, η is the learning rate, and θ_0 is randomly-initialized parameters.

B. Federated Learning

The unprecedented successes of deep learning heavily depend on a massive amount of available data and training a model commonly requires centralizing the available data on one machine or a single data center [9]. Nonetheless, recently released data protection rules, e.g., General Data Protection

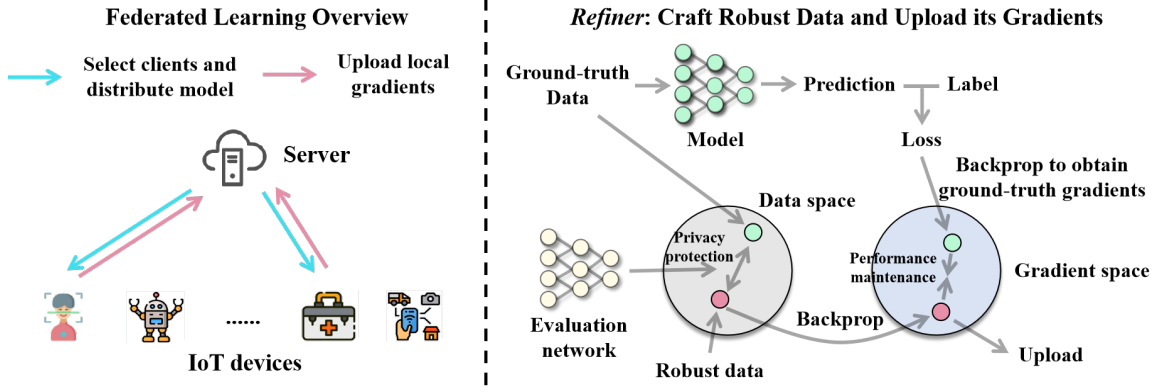


Fig. 1: Overview of *Refiner*. *Refiner* refines ground-truth data to craft robust data and the gradients of robust data are uploaded to the server. *Refiner* increases and decreases the distances of ground-truth data and robust data in data space and gradient space for performance maintenance and privacy protection, respectively.

Regulation in the European Union or Data Security Law of the People's Republic of China, explicitly forbid freely collecting user data to prevent abuse or privacy leakage, when without the grant of users. In this context, federated learning (FL) [9] emerges as a promising solution that can train a model without the requirement of centralizing user data. In vanilla FL, a server coordinates clients to collectively train a globally-shared model by alternatively implementing the below two steps for total T rounds:

- **Model Distribution and Local Training.** The server first samples a fraction of n clients out of all N clients to participate in t -th round while the others wait for the next round. $F(\cdot, \theta_{t-1})$ is distributed to the selected clients and these clients undergo training of the model on their local data in a pre-specified fashion to get ground-truth gradients. The produced ground-truth gradients in i -th selected clients is denoted by g_{t-1}^i and \hat{g}_{t-1}^i ($i = 1, \dots, n$) are uploaded to the server.
- **Global Aggregation.** Upon having received g_{t-1}^i ($i = 1, \dots, n$), the server averagely aggregates these gradients to update the global model to obtain $F(\cdot, \theta_t)$ for next round, i.e., $\theta_t = \theta_{t-1} - \eta \frac{1}{n} \sum_{i=1}^n g_{t-1}^i$.

Simply speaking, federated learning splits each normal iteration (Equation 1) into two steps where the gradient computation step is handed over to clients and the server only is in charge of model update step. This way creates a privacy-focused model training fashion, as the private data of clients is not necessary out of the local domains.

C. Threat Model

We assume that the server is honest-but-curious [16], i.e., the server adheres to the pre-defined training rules but is with a strong intention of revealing the training data of clients. To this end, before implementing the aggregation step, the server is always willing to leverage the uploaded gradients from a certain client to reconstruct training data of the corresponding client, i.e., launching GLA. Furthermore, the server can launch GLA against each client to steal corresponding training data,

since each client has a chance of being selected in a particular round and is then responsible to send the locally-computed gradients to the server. Notice that the server will honestly implement the aggregation step and thus this does not violate the pre-defined training rules.

We suppose that clients are alerted to the potential privacy leakage hazards and, as a remedy, clients are allowed to send perturbed gradients rather than ground-truth gradients [15], [16]. The perturbed gradients for i -th selected client in t -th round are denoted by \hat{g}_{t-1}^i . In the remainder of this paper, for notion simplicity, we omit the superscript and subscript, besides in some necessary statements.

D. Gradient Leakage Attack

The seminal work of gradient leakage attacks was proposed by [11], where the data can be reconstructed by solving gradient matching problems. With a certain optimization method, the server reconstructs client's data by forcing the gradients of randomly-initialized seed data x' with label y' to close uploaded gradients as possible:

$$x', y' = \arg \min_{x', y'} \|\nabla_{\theta} \mathcal{L}(F(x', \theta), y') - \hat{g}\|_2, \quad (2)$$

where \hat{g} is uploaded gradients and x' is reconstructed data. [12] discovered that the label can be explicitly recovered by observing the gradients of the fully-connected layer and attack effectiveness can be considerably improved by replacing y' with the ground-truth label. However, some works [13], [22], [23] empirically show that there are many feasible solutions in the image space for gradient matching problems and reconstructed images may be senseless. To address this problem, [13], [24] explored several useful regularization items like total variation to eliminate invalid reconstructions. Moreover, [22], [23] suggested some heuristic techniques, such as restart, and better initialization, that can make reconstruction easier. Recently, [18] assumed a threatening server that collects a lot of data similar to clients' data and trains a generative network to recover data. The generative network can narrow

the search space into manifolds where ground-truth data reside and therefore attack effectiveness is greatly enhanced.

E. Gradient Leakage Defense

Although cryptographic approaches, e.g., secure multiparty computation or homomorphic encryption, can be potential solutions for avoiding privacy leakage, the intrinsic overhead is too huge, making them hard to apply, as shown in [11], [16], [18]. Following [11], [16], [18], such methods are not discussed in this paper. [11], [17], [25] introduced differential privacy as a defense against GLA, where random noises are attached to ground-truth gradients to generate perturbed gradients. Besides, some works [15], [16] attempted to prune gradients to obfuscate the server and designed multiple different pruning strategies. For instance, [15] proposed Soteria that uses a theoretically-derived metric to evaluate the privacy info contained in gradient elements and then prunes gradients in fully-connected layers. However, Soteria has two significant limitations: 1) the gradients in fully-connected layers can be muted during the reconstruction process to break it [16], [17] and 2) the theoretically-derived metric depends on the one-order Taylor expansion of neural networks and this expansion seldom works well for neural networks. [16] solved the first limitation of Soteria but the second still exists, which is the major factor why only weak defense effectiveness of Soteria is presented in practice, especially when facing threatening server [17], [18].

III. APPROACH: *Refiner*

In this section, we detail *Refiner* that is outlined in Protocol 1 and Figure 1.

A. Overview of *Refiner*

The overall goal is to find proper \hat{g} that possess good utility while obfuscating the server to reconstruct false data. However, as suggested in Section I, directly optimizing gradients is infeasible, because of the difficulty in deriving the analytical gradient-to-data mapping. To respond to it, *Refiner* refines ground-truth data to craft robust data and the gradients of robust data replace ground-truth gradients to upload. Furthermore, if robust data and original data are significantly different, the server surely cannot reveal the original data. Now, given privacy preference level β and ground-truth data x with label y , the problem can be formulated as follows:

$$x^* = \arg \min_{x^*} UM(x^*, x) - \beta \cdot PM(x^*, x), \quad (3)$$

where x^* is crafted robust data and $UM(\cdot)$ and $PM(\cdot)$ denote our utility and privacy metrics, respectively. The utility metric is used to evaluate how much less utility x^* is compared to x , and the privacy metric indicates how much less privacy about x is contained in x^* . Guided by the two metrics, the gradients of resultant x^* will not only be instructive but also can effectively obfuscate the server. In the next two subsections, we will elaborate on the two metrics.

Protocol 1 Federated Learning with *Refiner*

Input: A model F with initialized parameters θ_0 ; total N clients with their local dataset and a server; the total rounds T ; the total refinement iterations I ; the mix factor α ; the balance factor β ;

- 1: **for** $t = 1$ to T **do**
- 2: **# Model Distribution.**
- 3: Select a subset of n clients out of all clients and distribute $F(\cdot, \theta_{t-1})$ to selected clients.
- 4: **# Local Training.**
- 5: **for** i -th selected client, $i = 1, 2, \dots, n$ **do**
- 6: Compute ground-truth gradients g_t^i associated with the i -th selected client's data x based on pre-defined training rules.
- 7: Sample v from uniform distribution and initialize robust data $x^* = (1 - \alpha)x + \alpha v$.
- 8: **for** $j = 1$ to I **do**
- 9: Compute $Loss = UM(x^*, x) - \beta \cdot PM(x^*, x)$ based on x^* , x , and g_t^i .
- 10: Update x^* with gradient descent algorithm by optimizing $Loss$.
- 11: **end for**
- 12: Compute gradients \hat{g}_t^i of x^* and upload \hat{g}_t^i to the server.
- 13: **end for**
- 14: **# Global Aggregation.**
- 15: Averagely aggregates the uploaded gradients \hat{g}_t^i , ($i = 1, 2, \dots, n$) and update θ_{t-1} to obtain θ_t .
- 16: **end for**
- 17: **Return** $F(\cdot, \theta_T)$.

B. Utility Metric (UM)

It is wished that UM can accurately estimate the gap of utility between x^* and x for the model, but, similar to identifying the gradient-to-data mapping relationship, the relationship of utility gap is intricate too [20]. Fortunately, notice that the parameters of the model are updated by gradients of loss function associated with specific data. Based on this, the distance between gradients of loss function with x^* and x can be taken as a proper proxy metric for the ground-truth utility metric.

The most commonly-adopted distance metric probably is mean square error (MSE) [21] and we also take advantage of it. However, it is not a wise option to directly leverage the original version of MSE for the following reason. The vanilla form of MSE equally treats any gradient elements involved and this suggests that exerting perturbations of the same magnitude into any gradient elements will cause losses of the same level. However, disturbing different gradient elements, even to the same extent, still produces resultant gradients of varying utility, since the parameters corresponding to different gradient elements own significantly different roles in model performance [20]. More detailed, perturbing gradient elements of critical parameters leads to higher loss than trivial

parameters.

In the light of the above insight, we customize a weighted MSE as proxy metric to make better alignment with the ground-truth utility metric. The overall idea of weighted MSE is to endow the gradients of important parameters with higher weights, which enables perturbing the gradients of important parameters more carefully and decreases loss in model performance. Two factors are taken into account here to determine the weights: statistical indicators of parameters, such as gradients, along with location information of parameters. In more detail, we define the element-wise weight by fusing statistical indicators of parameters, and the layer-wise weight by using location information. The product of element-wise weight and layer-wise weight is used as the ultimate weight for the corresponding gradient element.

Observation 3.1: *The significance of parameters is highly related to their values and gradients [26]. Intuitively, parameters with high magnitude values are crucial, since the parameters considerably reinforce their inputs compared to parameters with low magnitude values and higher outputs probably have more impact on model prediction; Besides, the nature of gradient is estimating the influence of a slight change in parameters on the final output and, thereby, parameters with gradients of high magnitude also play a critical role in model prediction.*

Element-wise Wight. Based on Observation 3.1, the element-wise weight can be defined as the absolute value of the product between value and gradient of a parameter. In fact, the values of parameters reflect their significance to upstream layers, and gradients of parameters suggest their importance to downstream layers, either should not be omitted in evaluating the weight. For instance, when only gradient information is hired, the value of the parameter is neglected. However, the parameter may be useless because the parameter is indeed inactivated if its value is near to zero.

To understand the element-wise weight further, we provide some math insights on it. Let $Q(\mu) = \mathcal{L}(F(x, \mu\theta), y)$. Then, there is $Q'(\mu) = \nabla \mathcal{L}(F(x, \mu\theta), y)^T \theta$. Notice that the optimal θ generally is reached when $\nabla \mathcal{L}(F(x, \theta), y) = 0$. We set μ to 1 and, consequently, $Q'(1) = \nabla \mathcal{L}(F(x, \theta), y)^T \theta$. If θ is optimal, $Q'(1) = 0$. Hence, we can check the value of $Q'(1)$ to judge whether optimality is obtained. In other words, if a parameter is with small magnitude value and gradient, it does not affect to obtain optimality.

Observation 3.2: *A neural network consists of many layers and each layer receives input from its adjacent upstream layer (except the input layer) and delivers its output to the adjacent downstream layer (except the output layer). As a result, the*

Some readers may be wondering how $Q(\mu)$ comes from. $Q(\mu)$ is a common mathematical practice in analysing optimality conditions of non-linear non-convex functions in high dimensional space. With this powerful tool, we can understand optimality conditions of complicated functions in a more intuitive way. We recommend interested readers refer [27] for more discussion about it. Moreover, notice that $Q'(1)$ only is the sufficient condition, not necessary condition, for best solution, but this does not impact us to use it.

earlier layers are probably more significant than the latter layers [26]. On the one hand, the errors induced by interfering with the learning process of earlier layers are likely to be intensely enlarged along with the forward propagation. On the other hand, a widely-known fact is that earlier layers typically concentrate on identifying bottom features shared across various samples, and therefore disrupting the learning process of earlier layers will make huge degradation in model performance.

Layer-wise Wight. Based on Observation 3.2, a sensible approach is to amplify the punishment on the perturbing of the gradients belonging to earlier layers, which allocates more attention to maintaining the gradients in earlier layers. Suppose that $F(x, \theta)$ have K layers in total and the i -th layer of $F(x, \theta)$ is parameterized with $\theta[i]$ ($\theta = \{\theta[1], \theta[2], \dots, \theta[K]\}$). The layer-wise wight of gradient elements in i -th layer $\theta[k]$ is defined as $power(\tau, i)$, where τ is decay factor ($0 \leq \tau \leq 1$) and $power(\cdot, \cdot)$ is power function.

Ultimate Weight. Here we formulate the ultimate weight for $\theta[i]$, which is product between element-wise weight and layer-wise weight:

$$weight(\theta[i]) = |grad(\theta[i]) \cdot value(\theta[i]) \cdot power(\tau, i)|, \quad (4)$$

where $grad(\theta[i])$ and $value(\theta[i])$ denotes taking out the gradients associated with $\theta[i]$ and values of $\theta[i]$. UM now can be defined as follows:

$$UM(x^*, x) = \left\| \sum_{i=1}^K weight(\theta[i]) (\nabla_{\theta[i]} \mathcal{L}(F(x^*, \theta), y) - grad(\theta[i])) \right\|_2^2. \quad (5)$$

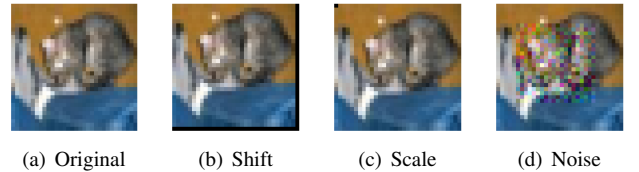


Fig. 2: We use three different methods to perturb the original image, shifting the original image towards the top-left direction by a unit, scaling a pixel of the original image, and adding random noises to the original image. However, compared with adding noises, shifting and scaling can yield higher MSEs, but with negligible privacy protection. Three methods make MSEs of 0.025, 0.106, and, 0.004, respectively.

C. Privacy Metric (PM)

PM is a distance metric that is used to quantify how much privacy about x is exposed induced by x^* , or how different x and x^* are from one another. Although there are many distance metrics, e.g., MSE, none of them are suitable as PM for our case. The reason for it is that these metrics are only intended to guarantee the high similarity between two inputs when the metrics associated with the two inputs fall within a low-value

range. Moreover, the inverse conclusion not always holds, i.e., two highly-similar images may be deemed to be different by these metrics, as shown in Figure 2. If the metrics are employed by *Refiner*, pseudo privacy protection senses may occur, since the metrics permit that the area with low losses includes such x^* that is similar to x .

Before proposing PM used in *Refiner*, we first state the property PM need. PM should possess the property: with the increasing value of PM, the privacy info contained in x^* should decrease monotonously. A straightforward idea for designing such PM is to craft a reference sample for x , and the reference sample does not contain any privacy info x . Subsequently, the distance between the reference sample and x^* can be used as PM. The lower the distance between x and the reference sample, the fewer the privacy of x contained in x^* is. However, it is quite cumbersome to search reference samples for each data. A better option is to craft a reference sample suitable across all data, and, obviously, a noise data is a appropriate choice. Specifically, we sample a noise data as a general reference sample from uniform distribution .

Even though the above way is doable, it remarkably restricts the overall performance of *Refiner*, because the search space is limited to the underlying route from x to the extracted fixed reference sample. In other words, the resultant x^* is likely to be near the extracted reference sample and this becomes the bottleneck of the performance of *Refiner*, due to some ones around other noises may being more instructive. Actually, it does not matter which random noises are extracted as the reference sample, as all random noises do not involve privacy info of x . Therefore, a better practice is to define the distance from x^* to noise distribution, i.e., distribution distance, as PM rather than a specific noise data. The distribution distance can be regarded as expanding the amount of reference samples available in the optimization process and x^* can be automatically guided to move forwards in a more informative reference sample direction, breaking through the bottleneck mentioned.

In practice, an evaluation network is employed to assess the proximity degree of x^* to noise distribution. The evaluation network is a neural network with output range of 0 to 1. Besides, outputting 1 indicates the input fully belonged to noise distribution and vice versa. The theory behind the network is maximum mean discrepancy (MMD) and MMD is a famous statistical concept that is frequently used to test whether two samples come from the same distribution [27]. Formally, MMD is as follows:

$$MMD(f, p, q) = \sup_{\|f\|_H \leq 1} E_{x \sim q(x)}[f(x)] - E_{x \sim p(x)}[f(x)], \quad (6)$$

where f is the evaluation network, $q(x)$ is noise (uniform) distribution, and $p(x)$ is data distribution of IoT devices. This suggests that we are required to train the network f to widen the expected output difference between $p(x)$ and $q(x)$ as much as possible. Furthermore, owing to the output of the

network being restricted to 0~1, widening the expected output difference essentially amounts to encourage the network to output 0 for ground-truth data x and 1 for noises separately.

Apart from the above, there is two points to be highlighted. To begin, during the training process of the network, we create training data-label pairs for the network in a interpolate manner, i.e., $((1-r) \cdot t_1 + r \cdot t_2, r)$, $r \sim U(0, 1)$, $t_1 \sim p$, $t_2 \sim q$, and these data-label pairs are supplied into the network as supervised signals. The benefit of doing so is that, the monotonicity principle, we suggest earlier, can be explicitly infused into the training process, since the knowledge that the output should be increased as r (the proportion of noise) rises is informed to the network. Secondly, we add gradient punishment during training process of the evaluation network to establish $\|f\|_H \leq 1$ [29]. Finally, the output of the trained evaluation network to x^* is adopted as PM, i.e., $PM(x^*, x) = f(x^*)$.

D. Solving the Optimization Task

Having the concrete forms of *UM* and *PM*, the remaining difficulty is figuring out how to solve Equation 3. In our case, the gradient descent algorithm is applied to iteratively solving Equation 3 with total iterations I , called refinement iterations. However, directly applying the gradient descent algorithm is problematic, due to the adversarial vulnerability of neural networks [30].

Observation 3.3: *The term "adversarial vulnerability" refers to this ubiquitous phenomenon: neural networks are vulnerable to adversarial examples, that can induce a huge shift in model prediction by adding subtle human-imperceptible noises into the original sample.*

Based on Observation 3.3, the resulting x^* by directly employing the vanilla gradient descent algorithm is extremely similar to x in semantics, i.e., x^* is the adversarial example of the evaluation network f . Adversarial examples can be considered as the local extreme points around x and an approach to address the problem is perturbing the initialization point to evade the area with local extreme points [31]. Accordingly, we initialize x^* with a mixture of x and random noises, i.e., $x^* = (1 - \alpha)x + \alpha v$, $v \sim q(x)$, $\alpha \in [0, 1]$ where α is a mix factor. If α is set to be big, x^* is initialized around the area flooding with noises, and the extreme point closest to x^* still is noises, thereby avoiding the adversarial vulnerability.

IV. EVALUATION

In this section, we conduct extensive experiments to evaluate the defense performance of *Refiner* compared with existing defenses.

A. Experiment Setup

Attacks. Four state-of-the-art attack methods are considered here to examine the defense performance of *Refiner*, i.e., iGLA [12], GradInversion [23], InvertingGrad [13], GGA [18]. These attacks differ primarily in the use of optimizer, regularization, and loss function, and Table I lists the details. We implement these attacks at the start of training since [17], [18], [22]

Uniform distribution is non-information distribution in information theory [28].

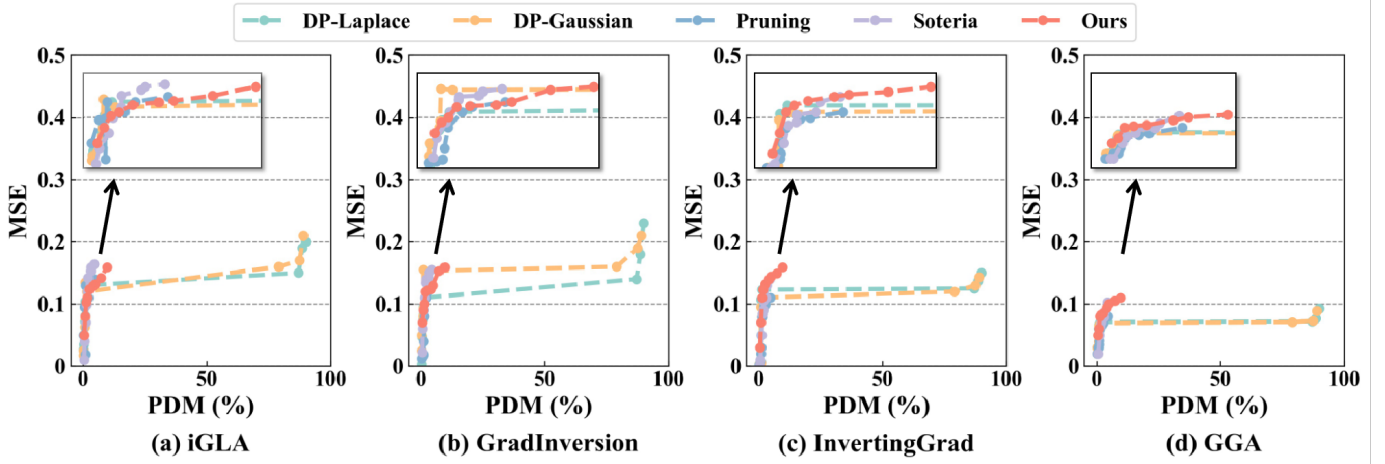


Fig. 3: The defense performance of five defenses against four different attacks in MNIST.

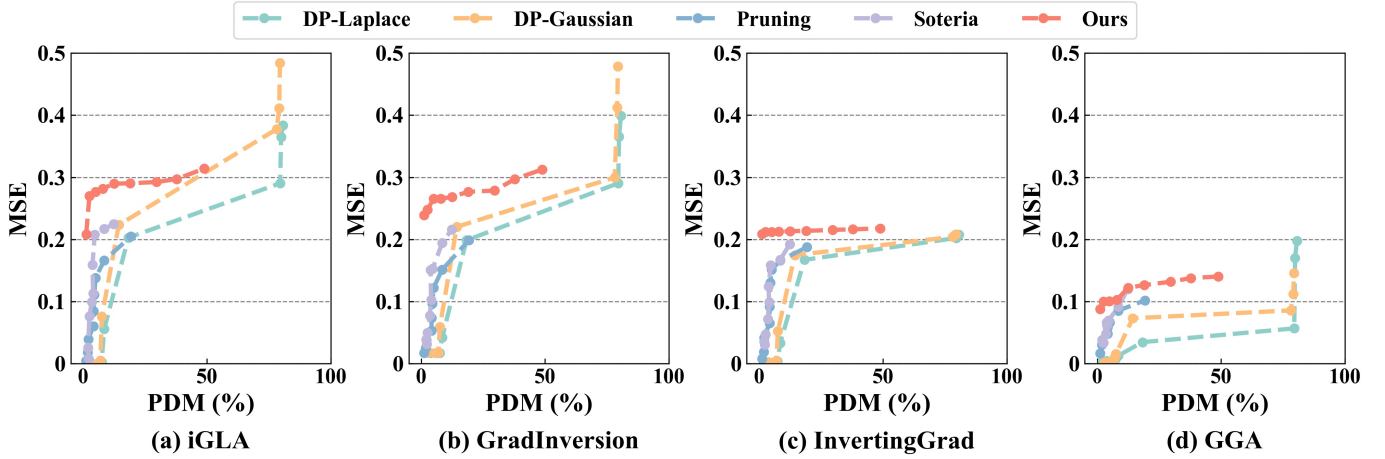


Fig. 4: The defense performance of five defenses against four different attacks in CIFAR-10.

TABLE I: Attack setting. The attack hyperparameters used in this paper follow their original papers. Total variance (TV) quantifies the smoothness of inputs and can be used to enhance the quality of recovered images. L_2 -norm controls the pixel value within a legal range $[0 \sim 255]$. BN statistics force the statistics of recovered images to close statistics of datasets. KL distance restricts the latent variables to follow Gaussian distribution.

Attack	iGLA	InvertingGrad	GradInversion	GGA
Gradient Loss	Euclidean	Cosine Similarity	Euclidean	Euclidean
Regularization	None	TV	TV+ L_2 -norm	GAN
Optimizer	L-BFGS	Adam	Adam	Adam
Learning rate	1	0.01	0.01	0.01
Label Inference	TRUE	TRUE	TRUE	TRUE
Attack Iteration	300	4000	4000	4000

suggests the stage is the most vulnerable against attacks. For GGA, we use public codes to train a GAN.

Competitors. Similar to [15], we compare our method *Refiner* with following defense methods: 1) differential privacy (DP) [14] injects a certain random noises to ground-truth gradients to produce uploaded gradients, 2) pruning [11] and Soteria [16] discards a part of gradient elements. For DP, we employ two different and common kinds of noises, namely Gaussian (DP-Gaussian) and Laplace (DP-Laplace), with magnitude $\{10^{-6}, 10^{-5}, \dots, 10^2\}$. For pruning and Soteria, we set pruning ratio in $\{0.1, 0.2, \dots, 0.9\}$. Besides, we discover α to be the most significant hyperparameters for the performance of *Refiner* and we alter α over $\{0.1, 0.2, \dots, 0.9\}$ to compare. If not otherwise specified, β , refinement iterations, and τ is set to 1, 100, 0.95 by default. Each IoT device trains an evaluator network with its local dataset for 20 epochs to conduct *Refiner*.

Evaluation metrics. We quantify the defense performance from two perspective [15]: performance maintenance and privacy protection. For performance maintenance, we leverage

We use Soteria proposed in [16] to compare, which is an improved version compared with the original Soteria [15].

performance degradation metric (PDM) that is defined as follows:

$$PDM = \frac{original_acc - defense_acc}{original_acc} \times 100\%,$$

where *original_acc* and *defense_acc* denote the accuracy of the model with and without defense. For privacy protection, we adopt MSE which measures the distance from reconstructed data to original data. In summary, the lower the PDM, the higher the MSE, and the better the defense.

Training setting. Following [15], all experiments are conducted on two benchmark datasets MNIST and CIFAR-10. We assume that there are 10 IoT devices. MNIST and CIFAR-10 consist of 50000 training data and 10000 test data and training data are evenly allocated among these devices. In each round, all devices are selected to compute local gradients with 128 training data and upload to the server. The server averagely aggregates the uploaded gradients and updates the global model with SGD optimizer of 0.01 learning rate. By default, the total rounds are set to 200 and 1000 for CIFAR-10 and MNIST [15], respectively.

B. The Evaluation of Refiner

In this subsection, we numerically compare the performance of the different defenses, followed by a visualization comparison.

Numerical results. Figure 3 and Figure 4 show the performance (in terms of MSE and PDM) of different defenses with varying hyperparameters against four threatening attacks in MNIST and CIFAR-10, respectively. A general observation is that, *Refiner* consistently achieves better defense performance compared with other defenses, as evidenced by higher MSE under comparable PDM, in CIFAR-10. Wherein, it is most surprising that the reconstructed images are quite different from the original ones, with the measured $MSE \geq 0.1$ across almost all cases. This implies that our defense, even with small defensive magnitude hyperparameters still can significantly mitigate existing attack methods on negligible degradation of model performance; whereas, other defenses struggle to prevent these attacks from synthesizing high-quality images. For instance, as demonstrated in Figure 4, *Refiner* surpasses more than MSE of 0.2 defense effectiveness over all hyperparameter settings, and Soteria, the state-of-the-art defense in this domain, only comes close to MSE of 0.2 defense effectiveness, under the strongest defensive strength hyperparameter (0.9 pruning rate).

We also notice that 1) the fidelity of reconstructed images in MNIST is usually better than CIFAR-10, and 2) the performance of *Refiner* is a little weaker than Soteria in MNIST against two attacks, iGLA and GradInversion. For the former one, we speculate that the phenomenon is caused by the that CIFAR-10 is a more sophisticated dataset than MNIST. Generally speaking, complicated images commonly demand more parameters to serve them for obtaining good prediction, and this suggests that the reconstruction of complicated images necessitates high-fidelity gradients because each gradient

element is not trivial. In contrast, simple images only use a few parameters, suggesting it is not sensitive to gradients of most parameters and needs more significant gradient perturbations to defend. Therefore, the same level gradient perturbations can result in more noticeable changes in CIFAR-10. For the latter one, this is attributed to iGLA and GradInversion being relatively weak attacks than InvertingGrad and GGA, considering the attack effectiveness of InvertingGrad and GGA are tremendously better than iGLA and GradInversion showed in Figure 3 and Figure 4. As such, the ground-truth defensive performance of Soteria is overestimated.

Visualization results. We now turn to visualization analysis which is a more intuitive way of perceiving the effectiveness of different defenses and Figure 5 presents images recovered by InvertingGrad and GGA under various defenses with varying hyperparameters. Due to the numerical performance superiority of *Refiner* presented before, an anticipation is that, it is hard to recover high-quality images that are similar to the original ones by employing gradients produced by *Refiner* with any legitimate α , and this is verified in Figure 5. Overall, *Refiner* can always obfuscate the server to reverse senseless images; whereas, other defenses only can achieve comparable defense effectiveness when defensive magnitudes are allowed to be bigger but this also causes non-negligible losses in model performance. Moreover, although the reconstructed images by GGA are combinations of the semantic fragments, but the overall semantics of the combinations dramatically differ from the original ones.

C. A Closer Look on why Refiner Works

In this subsection, we explore why *Refiner* works.

Privacy Protection. Figure 6(a) presents the robust data crafted by *Refiner* over varying α for several randomly extracted images from the training dataset. As can be seen, all crafted robust data at least are meaningless for human vision. Recalling that the premise of reconstructing high-fidelity images is leveraging the accurate gradient-to-data mapping relationship. Furthermore, if the uploaded gradients are substituted by the gradients of the robust data, the reconstructed data should be robust (meaningless) data instead of ground-truth data. Moreover, if the premise is broken, the recovered images should be of low-quality. Therefore, *Refiner* can prevent the server to reconstruct high-fidelity images.

Performance maintenance. Intuitively, performance maintenance ability is negatively correlated with the gradient distance between robust data and ground-truth data. Guided by this, we record the ratio of the gradient distance in ground-truth gradients, i.e., noise ratio, and present it in Figure 6(b). Noise ratio can be simply regarded as the noise intensity imposed in the ground-truth gradients and, In fact, is a common tool to analyze the impact of the gradient perturbation method on model performance [7], [14]–[16]. We observe that, with increasing α , the noise ratio also raises, since higher α indicates a less proportion of ground-truth data in the initialization point, and more refinement iterations are required to decrease the gradient distance. Besides, with small

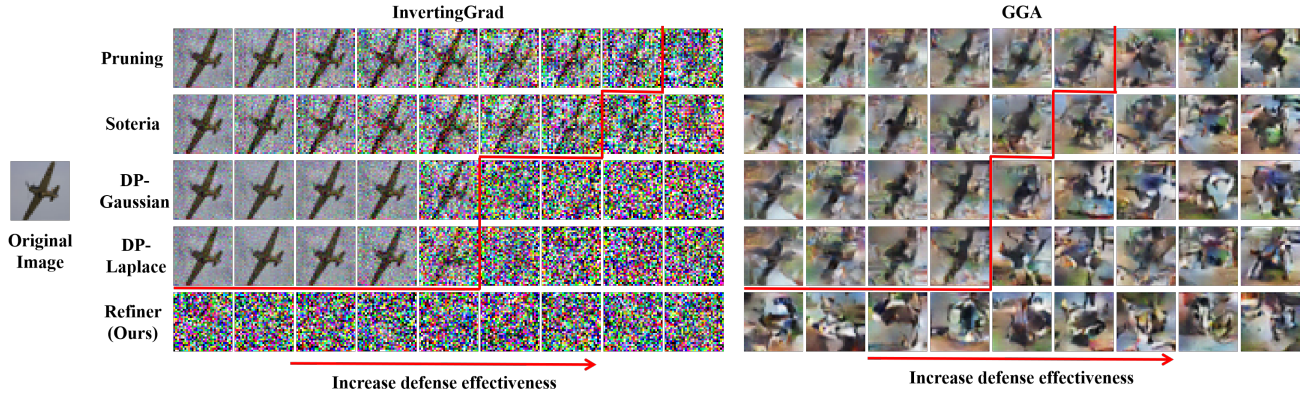
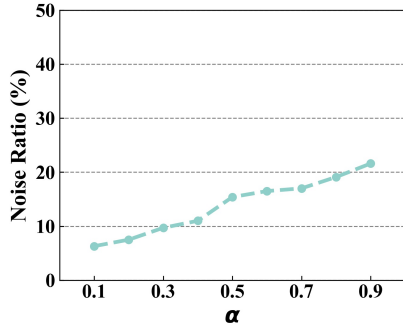


Fig. 5: A visualization of five defenses over different hyperparameters against two strong attacks, InvertingGrad and GGA, in CIFAR-10. The images above the red broken lines contain more or less privacy information of the original images.



(a) Robust Data



(b) Noise Ratio

Fig. 6: We randomly pick 5 images from the training set of CIFAR-10 and employ *Refiner* to craft robust data for each one under different hyperparameters (α increases along left to right). Additionally, we record the averaged noise ratio induced by robust data in each round over the entire training process in CIFAR-10.

α , e.g., $\alpha = 0.1$, the noise ratio is quite low, about 6%, and *Refiner* paid more attention to decreasing the gradient distance of critical parameters that are more important to model performance. Therefore, it is clear why *Refiner* can maintain model performance.

TABLE II: The defense performance of *Refiner* with α of 1 over β in MNIST and CIFAR-10 against InvertingGrad.

Dataset	Metric	0.001	0.01	0.1	1	10	100
MNIST	PDM	0.326	0.380	0.446	0.500	0.728	1.272
	MSE	0.022	0.024	0.029	0.030	0.047	0.056
CIFAR-10	PDM	0.541	0.972	1.110	1.210	4.961	12.485
	MSE	0.152	0.184	0.203	0.209	0.206	0.210

TABLE III: The defense performance of *Refiner* with α of 1 over different refinement iterations in MNIST and CIFAR-10 against InvertingGrad.

Dataset	Metric	1	5	10	20	50	100	200
MNIST	PDM	87.88	83.70	54.14	36.59	14.96	0.50	0.24
	MSE	0.011	0.013	0.017	0.019	0.024	0.030	0.080
CIFAR-10	PDM	70.17	66.99	64.68	19.50	4.02	1.21	0.51
	MSE	0.087	0.129	0.138	0.174	0.197	0.209	0.205

D. Sensitivity Analysis

In this subsection, we investigate the impact of hyperparameters on the performance of *Refiner*.

Impact of balance factor β . Table II reports the performance of *Refiner* as β varies against InvertingGrad. Overall, the higher β is, the greater model performance loss (PDM) is, and the higher MSE is. Moreover, the performance of *Refiner* is more robust to tuning β compared with α , i.e., there is not a huge performance shift w.r.t. different β . Thus, we believe setting $\alpha = 1$ by default is a good option in practice.

Impact of refinement iterations. Refinement iterations can greatly influence the quality of resultant robust data and Table III reports the performance of *Refiner* over different refinement iterations against InvertingGrad. A observation is that, the performance of *Refiner* intensively increases by raising refinement iterations from 1 to 100, but further enhancing refinement iterations from 100 to 200 only produce a slight improvement, suggesting that refinement iterations of 100 are sufficient for optimization convergence in practice.

V. CONCLUSION

In this study, we presented a novel yet effective gradient leakage defense called *Refiner*. Instead of directly perturbing ground-truth gradients, the fundamental idea of *Refiner* is to refine ground-truth data to obtain robust data that can produce similar utility but does not involve privacy info, compared with original ones. To do so, we formulated an optimization task to achieve it by optimizing two metrics for performance maintenance and privacy protection. In detail, we customized a weighted MSE as performance maintenance metric and designed an evaluation network as privacy protection metric. Finally, we conducted extensive experiments on MNIST and CIFAR-10 to verify the effectiveness of *Refiner* with the two metrics and *Refiner* achieve superior defense performance against state-of-the-art attacks.

REFERENCES

- [1] J. Steinberg, "These devices may be spying on you (even in your own home)," *Forbes*. Retrieved, vol. 27, 2014.
- [2] Y. Li, Y. Jiang, D. Tian, L. Hu, H. Lu, and Z. Yuan, "Ai-enabled emotion communication," *IEEE Network*, vol. 33, no. 6, pp. 15–21, 2019.
- [3] H. F. Nweke, Y. W. Teh, G. Mujtaba, and M. A. Al-Garadi, "Data fusion and multiple classifier systems for human activity detection and health monitoring: Review and open research directions," *Information Fusion*, vol. 46, pp. 147–170, 2019.
- [4] Geert, Litjens, Thijs, Kooi, Babak, Ehteshami, Bejnordi, Arnaud, Arindra, and Adiyoso, "A survey on deep learning in medical image analysis," *Medical Image Analysis*, 2017.
- [5] S. Gu, E. Holly, T. Lillicrap, and S. Levine, "Deep reinforcement learning for robotic manipulation with asynchronous off-policy updates," in *IEEE International Conference on Robotics & Automation*, 2017.
- [6] A. R. Sfar, E. Natalizio, Y. Challal, and Z. Chtourou, "A roadmap for security challenges in the internet of things," *Digital Communications and Networks*, vol. 4, no. 2, pp. 118–137, 2018.
- [7] X. He, F. Xue, X. Ren, and Y. You, "Large-scale deep learning optimizations: A comprehensive survey," *arXiv preprint arXiv:2111.00856*, 2021.
- [8] J. Mills, J. Hu, and G. Min, "Communication-efficient federated learning for wireless edge intelligence in iot," *IEEE Internet of Things Journal*, vol. 7, no. 7, pp. 5986–5994, 2019.
- [9] T. Li, A. K. Sahu, A. Talwalkar, and V. Smith, "Federated learning: Challenges, methods, and future directions," *IEEE Signal Processing Magazine*, vol. 37, no. 3, pp. 50–60, 2020.
- [10] D. C. Nguyen, M. Ding, P. Pathirana, A. Seneviratne, J. Li, and H. V. Poor, "Federated learning for internet of things: A comprehensive survey," *IEEE Communications Surveys & Tutorials*, 04 2021.
- [11] L. Zhu, Z. Liu, and S. Han, "Deep leakage from gradients," *Advances in Neural Information Processing Systems*, vol. 32, 2019.
- [12] B. Zhao, K. R. Mopuri, and H. Bilen, "idlg: Improved deep leakage from gradients," *arXiv preprint arXiv:2001.02610*, 2020.
- [13] J. Geiping, H. Bauermeister, H. Dröge, and M. Moeller, "Inverting gradients-how easy is it to break privacy in federated learning?" *Advances in Neural Information Processing Systems*, vol. 33, pp. 16 937–16 947, 2020.
- [14] M. Abadi, A. Chu, I. Goodfellow, H. B. McMahan, I. Mironov, K. Talwar, and L. Zhang, "Deep learning with differential privacy," in *Proceedings of the 2016 ACM SIGSAC conference on computer and communications security*, 2016, pp. 308–318.
- [15] J. Sun, A. Li, B. Wang, H. Yang, H. Li, and Y. Chen, "Soteria: Provable defense against privacy leakage in federated learning from representation perspective," in *Proceedings of the IEEE/CVF Conference on Computer Vision and Pattern Recognition*, 2021, pp. 9311–9319.
- [16] J. Wang, S. Guo, X. Xie, and H. Qi, "Protect privacy from gradient leakage attack in federated learning," in *IEEE INFOCOM 2022-IEEE Conference on Computer Communications*. IEEE, 2022, pp. 580–589.
- [17] M. Balunović, D. I. Dimitrov, R. Staab, and M. Vechev, "Bayesian framework for gradient leakage," in *International Conference on Learning Representations*, 2022.
- [18] Z. Li, J. Zhang, L. Liu, and J. Liu, "Auditing privacy defenses in federated learning via generative gradient leakage," in *Proceedings of the IEEE/CVF Conference on Computer Vision and Pattern Recognition*, 2022, pp. 10 132–10 142.
- [19] T. Hoefer, D. Alistarh, T. Ben-Nun, N. Dryden, and A. Peste, "Sparsity in deep learning: Pruning and growth for efficient inference and training in neural networks," *J. Mach. Learn. Res.*, vol. 22, no. 241, pp. 1–124, 2021.
- [20] S. Pouyanfar, S. Sadiq, Y. Yan, H. Tian, Y. Tao, M. P. Reyes, M.-L. Shyu, S.-C. Chen, and S. S. Iyengar, "A survey on deep learning: Algorithms, techniques, and applications," *ACM Computing Surveys (CSUR)*, vol. 51, no. 5, pp. 1–36, 2018.
- [21] J. L. Suárez, S. García, and F. Herrera, "A tutorial on distance metric learning: Mathematical foundations, algorithms, experimental analysis, prospects and challenges," *Neurocomputing*, vol. 425, pp. 300–322, 2021. [Online]. Available: <https://www.sciencedirect.com/science/article/pii/S0925231220312777>
- [22] W. Wei, L. Liu, M. Loper, K.-H. Chow, M. E. Gursoy, S. Truex, and Y. Wu, "A framework for evaluating client privacy leakages in federated learning," in *European Symposium on Research in Computer Security*. Springer, 2020, pp. 545–566.
- [23] H. Yin, A. Mallya, A. Vahdat, J. M. Alvarez, J. Kautz, and P. Molchanov, "See through gradients: Image batch recovery via gradinversion," in *Proceedings of the IEEE/CVF Conference on Computer Vision and Pattern Recognition*, 2021, pp. 16 337–16 346.
- [24] J. Jeon, K. Lee, S. Oh, J. Ok *et al.*, "Gradient inversion with generative image prior," *Advances in Neural Information Processing Systems*, vol. 34, pp. 29 898–29 908, 2021.
- [25] W. Wei, L. Liu, Y. Wut, G. Su, and A. Iyengar, "Gradient-leakage resilient federated learning," in *2021 IEEE 41st International Conference on Distributed Computing Systems (ICDCS)*. IEEE, 2021, pp. 797–807.
- [26] Y. Cheng, D. Wang, P. Zhou, and T. Zhang, "Model compression and acceleration for deep neural networks: The principles, progress, and challenges," *IEEE Signal Processing Magazine*, vol. 35, no. 1, pp. 126–136, 2018.
- [27] S. Theodoridis, *Machine learning: a Bayesian and optimization perspective*. Academic press, 2015.
- [28] F. M. Reza, *An introduction to information theory*. Courier Corporation, 1994.
- [29] J. Adler and S. Lunz, "Banach wasserstein gan," *Advances in neural information processing systems*, vol. 31, 2018.
- [30] I. J. Goodfellow, J. Shlens, and C. Szegedy, "Explaining and harnessing adversarial examples," *Computer Science*, 2014.
- [31] E. Wong, L. Rice, and J. Z. Kolter, "Fast is better than free: Revisiting adversarial training," in *International Conference on Learning Representations*, 2019.